Journal of Hazardous Materials 174 (2010) 416–423

Contents lists available at ScienceDirect

Journal of Hazardous Materials

journal homepage: www.elsevier.com/locate/jhazmat

Calculated flame temperature (CFT) modeling of fuel mixture lower flammability limits

Fuman Zhao, William J. Rogers, M. Sam Mannan*

Mary Kay O'Connor Process Safety Center, Department of Chemical Engineering, Texas A&M University, College Station, TX, 77843-3122, United States

ARTICLE INFO

Article history:
Received 11 May 2009
Received in revised form
12 September 2009
Accepted 14 September 2009
Available online 20 September 2009

Keywords:
Lower flammability limit
Fuel mixtures
Calculated flame temperature
Energy conservation

ABSTRACT

Heat loss can affect experimental flammability limits, and it becomes indispensable to quantify flammability limits when apparatus quenching effect becomes significant. In this research, the lower flammability limits of binary hydrocarbon mixtures are predicted using calculated flame temperature (CFT) modeling, which is based on the principle of energy conservation. Specifically, the hydrocarbon mixture lower flammability limit is quantitatively correlated to its final flame temperature at non-adiabatic conditions. The modeling predictions are compared with experimental observations to verify the validity of CFT modeling, and the minor deviations between them indicated that CFT modeling can represent experimental measurements very well. Moreover, the CFT modeling results and Le Chatelier's Law predictions are also compared, and the agreement between them indicates that CFT modeling provides a theoretical justification for the Le Chatelier's Law.

1. Introduction

The knowledge of the lower flammability limit (LFL) is one of the primary parameters for the prevention of fire and explosion in industrial processes [1]. As with most aspects of flammability, the evaluation of flammability limits is not absolute, but rather depends on the details of the test apparatus and experimental conditions. In practice, flammability limits are affected by a variety of factors including temperature, pressure, different oxygen concentration, inert gas addition, size and shape of equipment, and direction of flame propagation [2].

Two hundred years of flammability limit experiments have shown that flammability limits are dependent on the size and configuration of the experimental apparatus [3]. Coward and Jones [4] used a cylindrical vertical tube of 5 cm diameter to measure the flammability limits for a wide variety of gases and vapors. Later, Zabetakis [5] suggested that a tube diameter of 5 cm is too small for accurate measurement of the flammability of some flammable halogenated hydrocarbons. An experimentally determined lower flammability limit of a methane/air mixture in 24 mm diameter tube was $4.90 \pm 0.03\%$ by volume, compared with the earlier measured flammability limit of 5.1–5.2% in a standard tube [6]. Takahashi et al. [7] evaluated the flammability limit changes with apparatus of different geometry, and pointed out that the flammability limits at ambient conditions are primarily determined by the quenching effect of the wall for a cylindrical vessel particularly with a small diameter and a large height.

Together with structural group contribution (SGC) modeling [8], calculated adiabatic flame temperature (CAFT) modeling [9,10] is a popularly used method to estimate lower flammability limits by assuming a temperature threshold or calculated adiabatic flame temperature. By using the methodology developed by Vidal et al. [10], the lower flammability limit can be computed as a function of the calculated adiabatic flame temperatures. However, disparities appeared when comparing predictions from CAFT modeling with experimental observations using different flammability apparatus [3]. Because CAFT modeling is an ideal approach with the assumption of the adiabatic conditions, evaluation of experimental data using this modeling requires the consideration of heat losses from flammability apparatus, especially for those with significant quenching effects.

In this research, an apparatus-related flame temperature model, or calculated flame temperature (CFT) modeling, is constructed based on the mass and energy balances in a certain cylindrical reaction vessel, where heat loss is taken into account as an indispensable part of the energy conservation equation. The lower flammability limits of hydrocarbon mixtures (methane and propane, methane and *n*-butane, methane and ethylene, ethylene and propylene, and ethylene and acetylene) are estimated by applying CFT modeling. To verify the validity of this model, the modeling results are compared with experimental observations. Because Le Chatelier's Law provides a simple way to estimate lower flammability limits of fuel mixtures, the results obtained with CFT modeling are compared to the computed results with Le Chatelier's Law.

* Corresponding author. Tel.: +1 979 862 3985.
E-mail address: mannan@tamu.edu (M.S. Mannan).

0304-3894/$ – see front matter © 2009 Elsevier B.V. All rights reserved.
doi:10.1016/j.jhazmat.2009.09.069

Nomenclature

A_s	surface area (m^2)
C_C	correction factor for carbon dioxide
C_W	correction factor for water vapor
C_{V_j}	constant volume heat capacity for species j ($kJ\,mol^{-1}\,K^{-1}$)
D_{in}	inside diameter (m)
ΔE_c	energy of combustion (J)
h_{in}	heat convection transfer coefficient at inside surface of the reactor ($W\,K^{-1}\,m^{-2}$)
ΔH_c	enthalpy of combustion (J)
k	thermal conductivity ($W\,m^{-1}\,K^{-1}$)
L	flame propagation distance from ignition source to thermistor 5 (m)
LFL	lower flammability limit (vol%)
n_j	molar number for species j (mol)
Δn	molar number change for a certain reaction (mol)
Nu	Nusselt number
P_0	initial pressure (Pa)
Q	heat exchange (J)
$\widetilde{Q}$	total heat losses per molar fuel (J/mol)
Q_c	heat convection (J)
$Q_{c,\,in}$	heat convection at the inside surface of the reactor (J)
Q_r	heat radiation (J)
$Q_{r,\,in}$	heat radiation at the inside surface of the reactor (J)
Q_T	total heat losses (J)
R	universal gas constant ($8.314\,J\,mol^{-1}\,K^{-1}$)
R_{in}	inner radius of the reactor (m)
Δt	flame propagation duration (s)
T_∞	ambient temperature (K)
T_f	final flame temperature (K)
T_0	initial temperature (K)
T_{in}	temperature at the inside surface of the reactor (K)
U_f	final internal energy (J)
U_i	initial internal energy (J)
ΔU	internal energy change (J)
V_g	volume of gas mixture in the region of flame propagation from ignition source to thermistor 5 at the initial temperature (m^3)
W	work (J)
x	fuel molar fraction

Greek letters

α	heat loss effectiveness factor
α_c	absorptivity for carbon dioxide
α_g	total gas absorptivity
$\bar{\alpha}_g$	average total gas absorptivity (1400–1600 K)
α_w	absorptivity for water vapor
$\Delta\alpha$	absorption overlap correction factor
ε_c	emissivity for carbon dioxide
ε_g	total gas emissivity
$\bar{\varepsilon}_g$	average total gas emissivity (1400–1600 K)
ε_w	emissivity for water vapor
$\Delta\varepsilon$	emission overlap correction factor
σ	Stefan-Boltzmann constant ($5.67 \times 10^{-8}\,W/m^2\,K^4$)
φ	molar fraction of a fuel or a fuel mixture consumed in the reactor

2. Experiment

The lower flammability limit data for pure fuels and fuel mixtures are measured through a flammability apparatus developed by Wong [11] at Texas A&M University. The flammability apparatus (Fig. 1) used in this research is a closed stainless steel (SS 316) cylindrical vessel with an internal diameter of 10.22 cm and 100 cm length. At the central line of the reaction vessel, there are five evenly-separated temperature sensors consisting of NTC thermistors (Thermometrics, FP07DB104N with fast response time 0.1 s in still air), which can monitor a self-sustained flame propagation when fuel/air premixed mixtures combust upwardly. Thermistor 1 is located at a distance of 15 cm from the ignition source (5 cm off the bottom surface of reaction vessel). The greatest distance from the ignition source to the farthest thermistor number 5 is 75 cm.

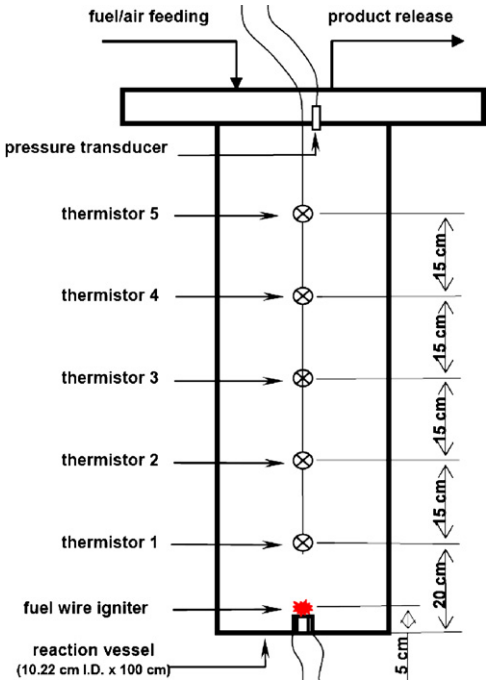

Fig. 1. Schematic diagram of the flammability apparatus.

A flame propagating 75 cm distance or over detected visually by thermistors is defined as continuous flame propagation [12]. The procedure to determine the lower flammability limit is according to the one developed by Wierzba et al. [13] that the probability of continuous flame propagation can vary from 0% to 100% when the fuel is within a certain concentration range near the lower flammability limits. At each fuel concentration, 10 tests are performed, and the number of times of the continuous flame propagation is recorded; therefore, the probability of continuous flame propagation is obtained at this selected concentration. Then, the probability of continuous flame propagation is plotted against fuel concentration, and by regression a linear line is obtained, on which a concentration with a 50% probability of continuous flame propagation is identified as the lower flammability limit of the measured fuel/air mixture [12]. Fig. 2 is an example, which illustrates the procedure to determine the lower flammability limit of methane in air. The experimentally determined lower flammability limits of pure methane are compared with some literature data from previous research using different experimental apparatus and detection criteria, and the data are shown in Table 1.

3. Theory and calculation

3.1. Theory of calculated flame temperature (CFT) modeling

The first law of thermodynamics is applied as a starting point for developing the CFT model (Eq. (1)), where ΔU is the change in

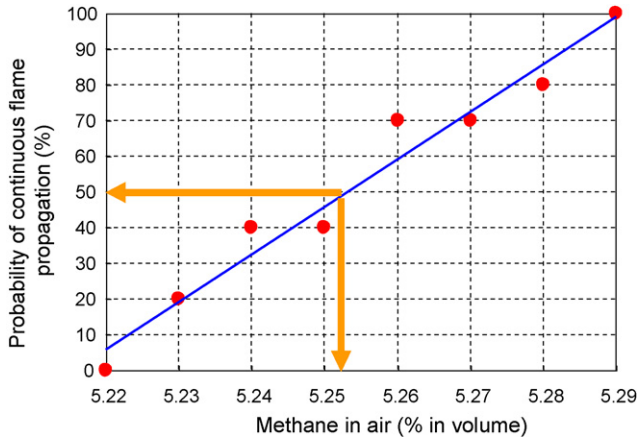

Fig. 2. Determination of the lower flammability limit of methane in air.

internal energy for a reaction system; U_f and U_i are the final and initial internal energy, respectively; W is work acting on the system and Q is the total amount of heat exchanged between the reaction gas and its surroundings.

$$\Delta U = U_f - U_i = W + Q \quad (1)$$

Heat exchange (Q) is dependent on the apparatus configuration, which is generally related to heat losses from burned gas to unburnt gas through heat convection (Q_c) and heat radiation (Q_r), and heat conduction is usually negligible in the combustion chamber. The internal energy change (ΔU) can be subdivided into two parts: internal energy change (ΔU_1) from fuel combustion at the initial temperature expressed as Eq. (2), and internal energy change (ΔU_2) from initial temperature (T_0) to final flame temperature (T_f) in Eq. (3). Combining Eqs. (1), (2) and (3), the final governing equation for CFT modeling is obtained as Eq. (4).

$$\Delta U_1 = \Delta E_c = \Delta H_c - \Delta nRT \quad (2)$$

$$\Delta U_2 = \sum_{\text{prods}} n_j \int_{T_0}^{T_f} C_{V_j} dT = f(T_f) \quad (3)$$

$$(\Delta H_c - \Delta nRT_0) + \sum_{\text{prods}} n_j \int_{T_0}^{T_f} C_{V_j} dT = (Q_c + Q_r) + W \quad (4)$$

where ΔE_c, ΔH_c are energy of combustion and enthalpy of combustion, respectively, which are empirically negative for exothermic combustion. Heat losses (Q_r, Q_c) from burnt gas to the surroundings are set to be negative. Work action on the reaction system is positive.

3.2. CFT modeling methodology

Building and application of CFT modeling involves a four-step procedure:

Table 1
Low flammability limits of pure methane in air (25 °C and 1 atm).

Methane LFL in air (%)	Apparatus types
5.3	Vertical glass cylinder
4.85	20 L sphere, 7% pressure rise
4.3	EN 1839 (T)
4.95	EN 1839 (B)
4.66	Counterflow burner
5.25 ± 0.05	This research

Table 2
Experimental lower flammability limits of pure fuels in air at standard conditions*.

Fuel	LFL (%)
CH_4	5.25(0.05)
C_3H_8	2.09(0.05)
n-C_4H_{10}	1.72(0.05)
C_2H_4	2.81(0.05)
C_3H_6	2.28(0.05)
C_2H_2	2.42(0.05)

* @ room temperature and 1 atm.

(i) Collecting pure fuel lower flammability limit data, which are specific to a certain apparatus;
(ii) Estimating the average flame temperature of the burned gas for pure fuels;
(iii) Estimating the average flame temperature of the burned gas for fuel mixtures;
(iv) Determining the lower flammability limits for the fuel mixtures.

3.2.1. Flammability limits of pure fuels

The lower flammability limit data for the pure fuels (methane, propane, n-butane, ethylene, propylene, and acetylene) were experimentally determined using a cylindrical flammability apparatus, as illustrated in the previous section. Table 2 gives the experimental results.

3.2.2. Flame temperatures of pure fuels

From the CFT governing equation, Eq. (4), a pure fuel's final flame temperature (T_f) can be calculated as a variable by estimating heat exchange (Q_c and Q_r), work done on the reaction system (W), energy of combustion at the initial temperature ($\Delta H_c - \Delta nRT_0$), and molar numbers n_j of the reaction product j.

3.2.2.1. Energy of combustion ($\Delta H_c - \Delta nRT_0$). At the concentration of lower flammability limit (oxygen is in excess), fuel reacts completely in air and most hydrocarbons have the flame temperature less than 1650 K, therefore the dissociation products can be negligible [14]. The enthalpy of combustion ΔH_c at initial temperature T_0 can be estimated from the thermodynamic data of the enthalpy of formation when combustion products only include CO_2 and H_2O. Δn is total mole number change in a certain chemical reaction. For a general hydrocarbon, C_aH_b, at lower flammability limit, the total molar change can be easily calculated by applying chemical reaction equation (Eq. (5)). R is the universal gas constant (8.314 J mol^{-1} K^{-1}). Table 3 lists the energy of combustion for the selected pure fuels (methane, propane, n-butane, ethylene, propylene, and acetylene).

$$C_aH_b + \frac{(1-\text{LFL})}{4.77 \times \text{LFL}}(O_2 + 3.77N_2) \rightarrow aCO_2 + \frac{b}{2}H_2O + \frac{3.77 \times (1-\text{LFL})}{4.77 \times \text{LFL}}N_2 + \left(\frac{1-\text{LFL}}{4.77 \times \text{LFL}} - a - \frac{b}{4}\right)O_2 \quad (5)$$

3.2.2.2. Work (W). Work acted on the reaction system W can be set to zero, because there are no volume work and no shaft work introduced into this system.

3.2.2.3. Heat losses (Q). For the cylindrical reaction apparatus, heat losses from the reaction system mainly involve convective and radiative heat transfer from combustion products and flame to the inside surface of the reaction vessel, followed by heat absorption and conduction in the vessel wall. Finally the thermal energy is

Table 3
Energy of combustion for pure fuels at standard conditions*.

Fuel	ΔH_c (kJ/mol-fuel)	Δn (mol/mol-fuel)	ΔnRT_0 (kJ/mol-fuel)	ΔE_c (kJ/mol-fuel)
CH_4	−802.3	0	0	−802.3
C_3H_8	−2043.1	1	2.48	−2045.6
n-C_4H_{10}	−2656.0	1.5	3.72	−2659.7
C_2H_4	−1323.1	0	0	−1323.1
C_3H_6	−1926.4	0.5	1.24	−1927.6
C_2H_2	−1255.5	−0.5	−1.24	−1254.3

* @ room temperature and 1 atm.

transferred away by natural convection and radiation from the outside surface of the vessel. Therefore, the total heat losses (Q_T) can be summarized as heat absorption into the vessel wall plus heat loss to the surroundings during flame propagation (starting from ignition of the fuel mixture at the ignition source, followed by upward flame propagation, and ending with flame exhaustion). Based on the principle of heat flux mechanism, the total heat losses can be represented as the summation of the net heat convection ($Q_{c,in}$) and the net heat radiation ($Q_{r,in}$) into the inside surface of the reaction vessel (Eq. (6)).

$$Q_T = Q_{c,in} + Q_{r,in} \tag{6}$$

The flame behavior in the cylindrical reaction vessel is particularly important to estimate the heat losses. Generally, as the fuel concentration approaches the flammability limit, the combustion becomes weak and the propagating flame only consumes a fraction of the fuel, which is strongly dependent on the geometry of the flammability apparatus. For the cylindrical apparatus and spherical apparatus, the former is more flame-favorable than the latter, or more fuel combusts in cylindrical vessels, especially for those with small diameters and large heights, e.g., the cylindrical reaction vessel used in this research. Thereby, the calculation of heat losses can be reasonably assumed as from heat source (burnt gas) to the inside vessel surface other than to the surrounding unburnt gas when the remaining unburnt gas is trivial compared to the burnt gas. Uncertainties from this assumption may be large, while they can be reduced by cancellation when we use the same assumptions to estimate heat losses from pure fuels and fuel mixtures. Meanwhile, axial heat losses are negligible compared with radial heat losses because of the big difference in surface area (the top and bottom surface area is about 3.4% of the side area) and heat loss tendency (the region of continuous flame propagation is 5 cm away from the bottom surface and 20 cm from the top surface).

The heat convection $Q_{c,in}$ can be calculated using Eq. (7)

$$Q_{c,in} = \alpha h_{in} 2\pi R_{in} L(T_f - T_{in})\Delta t \tag{7}$$

where R_{in} is the inside radius of the reaction vessel (5.11 cm), and T_f is the final flame temperature for a certain fuel. The inside surface temperature of the reactor, T_{in}, is set equal to the ambient temperature (T_∞ = 25 °C). L is the continuous flame propagation distance (75 cm from the ignition point to thermistor 5) from the flammability limit detection criterion applied in this research. α is the heat loss effectiveness factor. Along the propagating route of the premixed flame in the combustion chamber, four distinct zones can be identified: (i) the post-flame zone, which is characterized by high temperature and radical recombination with cooling occurrence subsequently; (ii) the reaction zone, in which most of the combustion takes place; (iii) the pre-heated zone attaching to the reaction zone, where the unburnt gases are heated; (iv) primary zone, in which temperature and concentration changes are negligible. At atmosphere pressure, the thickness of the reaction zone is quite thin with the order of millimeter [15]. Gaydon and Wolfhard identified that the thickness of the pre-heated zone is around 0.3 mm for the premixed flame at atmosphere pressure [16]. Thereby, the heat loss to the surroundings is mainly from the post-flame zone. Because fuel burning velocity is low at the concentration of lower flammability limit and self-sustaining flame propagates in a deflagration mode, a constant flame speed can be approximated, and the post-reaction zone will linearly expand. Thereby, 0.5 is set to the heat loss effectiveness factor. The flame propagation duration defined here as the time needed to cover the distance of L, Δt, can be theoretically estimated from the flame speed; however, calculation of flame speed would be extremely complicated because it depends on many parameters, e.g., fuel burning velocity, pressure (a closed combustion chamber used here), obstacles of the thermistors, and buoyancy and drag forces on fire ball. For simplicity, Δt is obtained from the experimental temperature profiles recorded by five thermistors and it is around 1 s (e.g., methane: 0.93 ± 0.1 s; propane: 0.93 ± 0.1 s; n-butane: 0.93 ± 0.1 s; ethylene: 1.06 ± 0.1 s; propylene: 1.06 ± 0.1 s; and acetylene: 0.87 ± 0.1 s). For general purpose, it is approximated to 1.0 (±0.1) s for the selected individual fuels. The heat convection coefficient at the inside surface of the reaction vessel, h_{in}, can be estimated using Eq. (8) [17] for a flame propagating through a premixed flammable mixture contained within a narrow, circular pipe of internal diameter D_{in},

$$h_{in} = Nu\ k/D_{in} \tag{8}$$

where, Nu = 3.65 for this configuration [18]. D_{in} = 10.22 cm for the cylindrical reaction vessel. k is thermal conductivity of the gas mixture, which can be approximated to air's thermophysical property at the lower flammability limits of the selected fuels (around 0.1 W/m K from 1400–1600 K [19]). Finally, h_{in} is obtained as 3.57 W/m^2 K.

The major contribution to heat loss due to radiation is the thermal radiation from water vapor and carbon dioxide in the burnt gas to the inside surface of the reaction vessel. Heat radiation emitted by the flame accounts for only a small portion of the total thermal radiation [20]. Therefore, the heat radiation loss, $Q_{r,in}$, can be characterized as the net radiation exchange between emission from the burnt gas to the inside black surface of the reaction vessel and *vice versa* (Eq. (9)).

$$Q_{r,in} = \alpha A_s \sigma(\varepsilon_g T_f^4 - \alpha_g T_{in}^4)\Delta t \tag{9}$$

where α is the heat loss effectiveness factor from thermal radiation, set to 0.5 based on the flame behavior indicated above. A_s is the reaction vessel surface area ($2\pi R_{in}L$), and σ is the Stefan-Boltzmann constant, 5.670×10^{-8} W/m^2 K^4. The average flame propagation duration Δt = 1 (±0.1) s. The total gas emissivity ε_g ($\varepsilon_g = \varepsilon_c + \varepsilon_w - \Delta\varepsilon$) can be estimated as a function of flame temperature T_f from the carbon dioxide emissivity ε_c, water vapor emissivity ε_w, and the radiation overlap correction factor $\Delta\varepsilon$. Similarly, total gas absorptivity α_g ($\alpha_g = \alpha_c + \alpha_w - \Delta\alpha$) can be quantified through the absorptivities of carbon dioxide α_c, water vapor α_w, and the correction factor $\Delta\alpha$ at the temperature T_{in} of the inside surface of the reaction vessel. The gas absorptivity can be evaluated from the gas emissivity (Eq. (10) for carbon dioxide, Eq. (11) for water vapor), and correction factors for emissivities and absorp-

Table 4
Average emissivities, absorptivities, overlap correction factors of carbon dioxide and water vapor at the temperature interval of 1400–1600 K and 1 atm.

Fuel	$\bar{\varepsilon}_c$	$\bar{\varepsilon}_w$	$\bar{\alpha}_c$	$\bar{\alpha}_w$	$\Delta\bar{\varepsilon}(\Delta\bar{\alpha})$	$\bar{\varepsilon}_g$	$\bar{\alpha}_g$
CH_4	0.025	0.013	0.054	0.038	0.011	0.027	0.081
C_3H_8	0.027	0.011	0.051	0.037	0.011	0.027	0.077
n-C_4H_{10}	0.028	0.011	0.064	0.032	0.011	0.028	0.085
C_2H_4	0.025	0.007	0.054	0.025	0.008	0.024	0.071
C_3H_6	0.028	0.009	0.063	0.030	0.010	0.027	0.083
C_2H_2	0.021	0.002	0.031	0.012	0.002	0.021	0.041

tivities are approximated to be equal ($\Delta\alpha = \Delta\varepsilon$) [19].

$$\alpha_c = C_c\left(\frac{T_f}{T_{in}}\right)^{0.65} \times \varepsilon_c \tag{10}$$

$$\alpha_w = C_w\left(\frac{T_f}{T_{in}}\right)^{0.45} \times \varepsilon_w \tag{11}$$

Table 4 lists the average emissivities $\bar{\varepsilon}$, average absorptivities $\bar{\alpha}$, and average overlap correction factors $\Delta\bar{\varepsilon}$ of carbon dioxide and water vapor for all the selected fuels at the temperature interval of 1400–1600 K. When fuel concentrations approach the lower flammability limits, all of these values are found to vary slightly within the selected temperature interval. By comparing the item $\varepsilon_g T_f^4$ with $\alpha_g T_{in}^4$, where ε_g and α_g are substituted for $\bar{\varepsilon}_g$ and $\bar{\alpha}_g$ Eq. (9) can be simplified to Eq. (12), because the value of $\bar{\alpha}_g T_{in}^4$ is much smaller than that of $\bar{\varepsilon}_g T_f^4$.

$$Q_{r,in} = \alpha 2\pi R_{in} L\sigma\bar{\varepsilon}_g T_f^4 \Delta t \tag{12}$$

Now, Eq. (13) can be simplified to convert the total heat losses (Q_T) in the reaction vessel to heat losses per mole fuel, which results in Eq. (14).

$$\widehat{Q} = \frac{(Q_{c,in} + Q_{r,in})RT_0}{LFL \times P_0 \times V_g} \tag{13}$$

$$\widehat{Q} = \frac{2\alpha RT_0\Delta t}{P_0\ LFL\, R_{in}}[h_{in}(T_f - T_{in}) + \sigma\bar{\varepsilon}_g T_f^4] \tag{14}$$

where LFL is the lower flammability limit of the pure fuels; V_g is the volume of the fuel/air mixture in the region of flame propagation from ignition source to thermistor 5 at the initial temperature ($\pi R_{in}^2 L$) and P_0 is the initial pressure in the vessel (1.01×10^5 Pa).

3.2.2.4. Molar numbers of the products. The molar numbers of the products, n_j, can be computed using the reaction equation (Eq. (5)). Table 5 shows the production amounts of the products (carbon dioxide, water, unchanged nitrogen, and the remaining oxygen) per molar pure fuel. Heat capacities for these products at constant volume are listed in Table 6. At room temperature and atmospheric pressure, it is reasonable to assume ideal conditions for all the fuel/air mixtures.

With all the available items shown above, the flame temperature can be estimated for each of the pure hydrocarbons by recalling the CFT model governing equation (Eq. (4)), which can become the function of the final flame temperature (T_f) specific to each of the pure fuels. The final CFT results for pure hydrocarbons are listed in Table 7.

Table 6
Heat capacities at constant volume C_v for combustion products (Eq. (5)).

Products	$C_v = a + bT + cT^2 + dT^3$ (J/mol K)			
	a	$b \times 10^2$	$c \times 10^5$	$d \times 10^9$
CO_2	13.929	5.977	−3.499	7.464
H_2O (g)	23.904	0.192	1.055	−3.593
N_2	20.569	−0.157	0.808	−2.971
O_2	17.146	1.519	−0.715	1.311

Table 7
Calculated flame temperature (CFT) and calculated adiabatic flame temperature (CAFT) at lower flammability limits of pure hydrocarbons.

Fuels	CFT T_F (K)	CAFT T_F (K)
CH_4	1628	1878
C_3H_8	1626	1870
n-C_4H_{10}	1680	1955
C_2H_4	1532	1727
C_3H_6	1661	1924
C_2H_2	1380	1521

3.3. Flame temperatures of fuel mixtures

Some previous research indicated that the pure fuels of hydrocarbons roughly have the same adiabatic flame temperature at the lower flammability limits [9,21]. Therefore, it is reasonable to assume that the adiabatic flame temperature is unchanged for fuel mixtures (combination of two or more hydrocarbons). However, for accurate lower flammability limit information, Vidal et al. [10] pointed out that the adiabatic flame temperatures for different fuels at lower flammability limits should be characterized separately. To estimate the adiabatic flame temperatures for fuel mixtures, Vidal et al. [10] proposed a linear equation which is represented in Eq. (15), where $T_{f,mix}^a$, $T_{f,1}^a$ and $T_{f,2}^a$ are the adiabatic flame temperatures of fuel mixtures, pure fuel 1 and pure fuel 2, respectively; and x_1, x_2 are the molar fractions ($x_1 + x_2 = 1$) of fuel 1 and fuel 2 in the fuel mixtures.

$$T_{f,mix}^a = x_1\ T_{f,1}^a + x_2\, T_{f,2}^a \tag{15}$$

Like the lower flammability limit, there exists a corresponding lower limit flame temperature for a pure fuel or fuel mixture, and below this threshold, a flame cannot propagate [9]. At adiabatic conditions, all generated energy is used to heat reaction products. However, when part of generated energy loses from reaction gas to the surroundings, more fuel is need to generate an extra heat to offset the lost heat, and the flame temperature still remain at the lower flammability limit flame temperature, or equals to the adiabatic flame temperature. Therefore, Eq. (15) can be extended to Eq. (16), where $T_{f,mix}$, $T_{f,1}$ and $T_{f,2}$ are final flame temperatures at

Table 5
Molar productions of reaction products (Eq. (5)) per mole of the pure hydrocarbons.

Fuel	n_j (mole/mole-fuel)			
	CO_2 (mol/mol-fuel)	H_2O (g) (mol/mol-fuel)	N_2 (mol/mol-fuel)	O_2 (mol/mol-fuel)
CH_4	1	2	14.26	1.78
C_3H_8	3	4	37.03	4.82
n-C_4H_{10}	4	5	45.16	5.48
C_2H_4	2	2	27.34	4.25
C_3H_6	3	3	33.87	4.46
C_2H_2	2	1	31.87	5.95

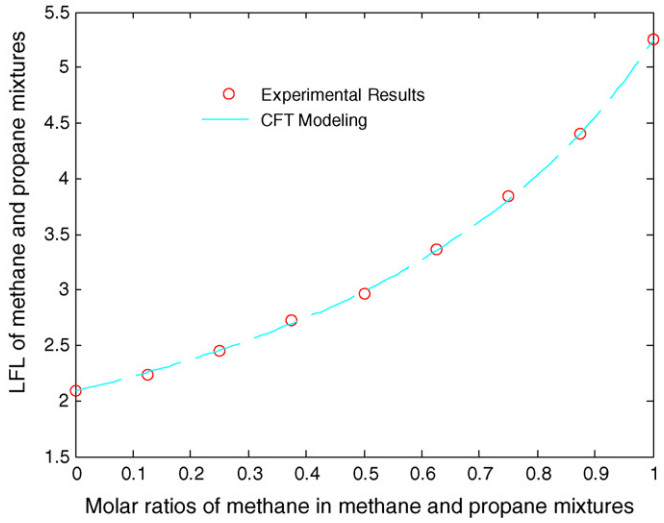

Fig. 3. LFL estimations for methane and propane mixtures using CFT modeling.

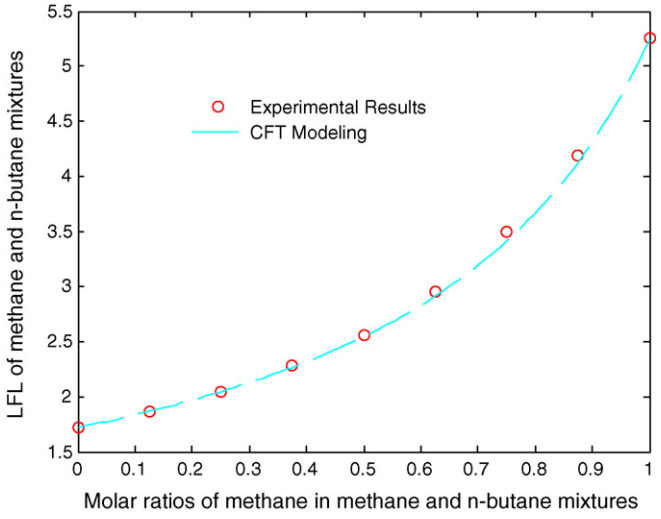

Fig. 4. LFL estimations for methane and *n*-butane mixtures using CFT modeling.

non-adiabatic conditions.

$$T_{f,mix} = x_1\ T_{f,1} + x_2\, T_{f,2} \tag{16}$$

3.4. Lower flammability limits of fuel mixtures

Finally, we apply the CFT model governing equation (Eq. (4)) again to estimate the lower flammability limits of binary hydrocarbon mixtures, where the heat losses are quantified using Eq. (14) with substitution of LFL_{mix} for LFL, $T_{f,mix}$ for T_f and $\bar{\varepsilon}_{g,mix}$ ($\bar{\varepsilon}_{g,mix} = x_1\bar{\varepsilon}_{g,1} + x_2\bar{\varepsilon}_{g,2}$) for $\bar{\varepsilon}_g$. Other parameters are assumed to be equal to those applied to a pure fuel. Because fuel mixtures combust completely at lower flammability limits, the energy of combustion ($\Delta E_{c,mix}$) can be calculated using Eq. (17) based on the Hess's Law of chemical reaction [22], which states that for the conversion from reactants to products, the change of energy is the same whether the reaction takes place in one step or in a series of steps. The molar productions of reaction products are obtained from the fuel mixtures' chemical reaction (Eq. (18)).

$$\Delta E_{c,mix} = x_1\Delta E_{c,1} + x_2\Delta E_{c,2} \tag{17}$$

$$[x_1 C_aH_b + x_2 C_mH_n] + \frac{(1-LFL_{mix})}{4.77LFL_{mix}}(O_2 + 3.77N_2) \rightarrow (ax_1 + mx_2)CO_2 + \frac{bx_1 + nx_2}{2}H_2O + \frac{3.77(1-LFL_{mix})}{4.77LFL_{mix}}N_2 + \left\{\frac{1-LFL_{mix}}{4.77LFL_{mix}} - (ax_1 + mx_2) - \frac{bx_1 + nx_2}{4}\right\}O_2 \tag{18}$$

The final results are illustrated in Figs. 3–7 for the binary hydrocarbon mixtures of methane and propane, methane and *n*-butane, methane and ethylene, ethylene and propylene, and ethylene and acetylene, respectively. The information presented in these figures indicates that the CFT modeling can represent the experimental results very well. Uncertainties of experimental lower flammability limits are around 0.05–0.07 vol% for all selected pure fuels and pure mixtures.

4. Discussion

Uncertainty is an important concern for CFT modeling. As mentioned above, estimation of heat losses is dependent on the flame behavior in the cylindrical reaction vessel. We assume all fuels combust in the region from ignition point to thermistor 5, while they

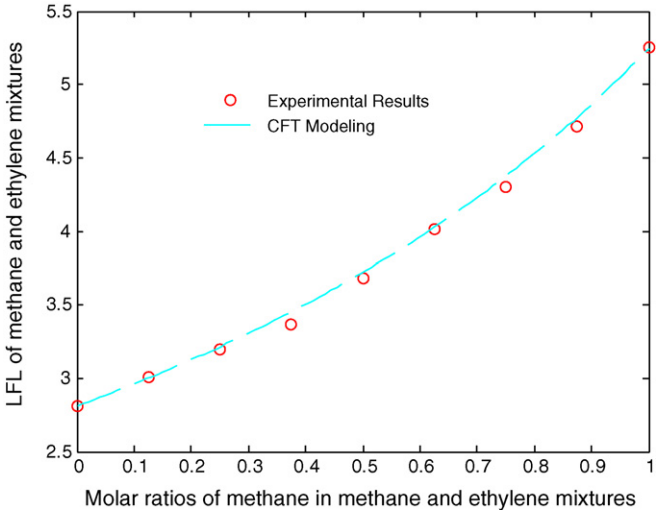

Fig. 5. LFL estimations for methane and ethylene mixtures using CFT modeling.

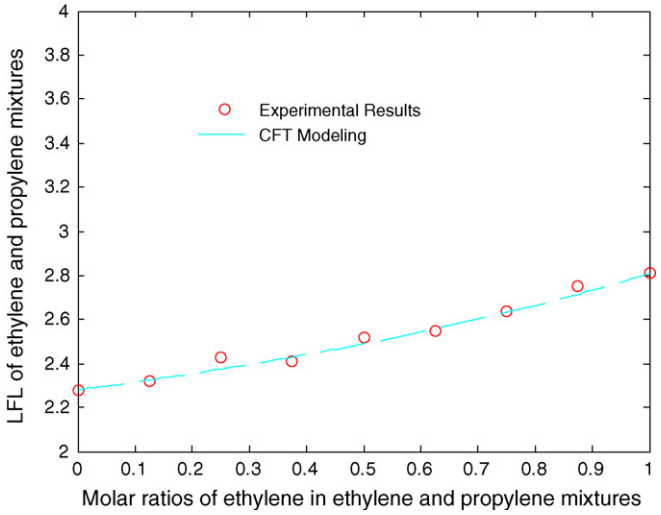

Fig. 6. LFL estimations for ethylene and propylene mixtures using CFT modeling.

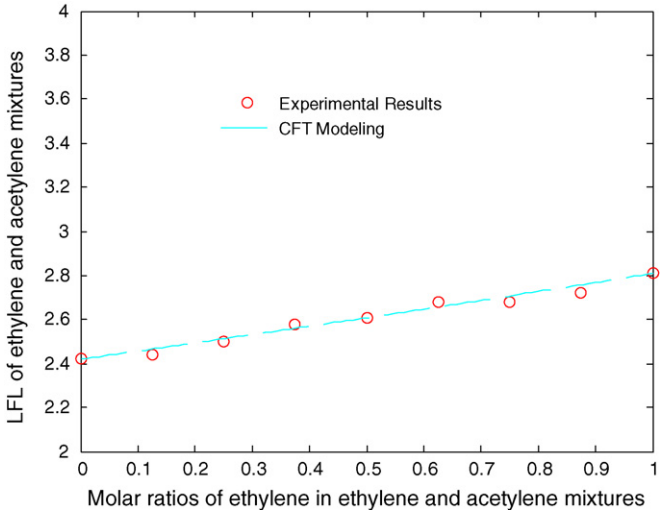

Fig. 7. LFL estimations for ethylene and acetylene mixtures using CFT modeling.

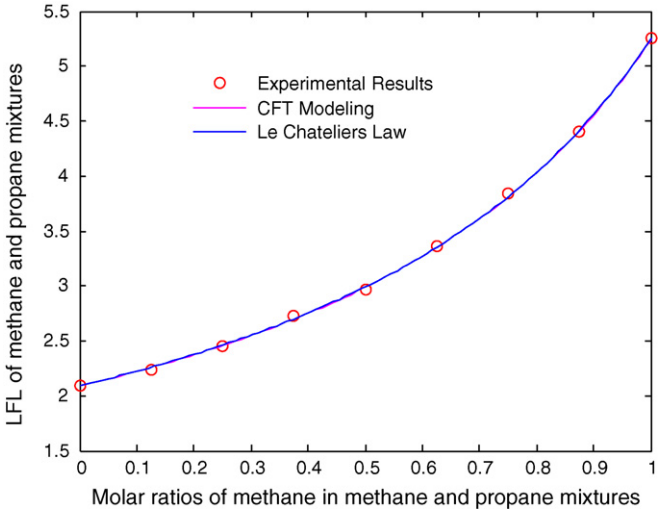

Fig. 8. LFL estimations for methane and propane mixtures using CFT modeling and Le Chatelier's Law.

do not in practice. We can imagine a certain fraction φ ($\varphi < 1$) of a fuel or fuel mixture is consumed at its lower flammability limit, e.g. φ_1 for fuel-1, φ_2 for fuel-2, and φ_{mix} for a certain combination of fuel-1 and fuel-2. The mixture fraction, φ_{mix}, is made up of φ_1 and φ_2. To some extent, uncertainty from the assumptions that are used to estimate heat losses, flame temperatures and the lower flammability limits of fuel mixtures can be reduced by cancellation between pure fuels and the fuel mixtures at the similar internal and external conditions. Also, uncertainties, which include thermophysical properties of pure fuels and fuel mixtures (e.g., heat convection coefficient h_{in}, heat conductivity k, and gas emissivity ε_g) and those from experimental observations (e.g., reaction vessel wall's surface temperature T_{in}, flame propagation time Δt, and heat loss effective factor α), can be reduced by cancellation between the pure fuels and fuel mixtures.

In reality, CFT modeling is a modification of CAFT modeling in which the phenomenon of heat loss is introduced. Whether CFT modeling overweighs CAFT modeling is dependent on heat loss tendency. When the quenching effect of a flammability apparatus becomes significant, CFT modeling is recommended because heat loss would be indispensable as a main factor to impact lower flammability limit estimation. If an adiabatic condition is presumed in the cylindrical flammability apparatus used in this research ($Q_r = Q_c = 0$), the estimated calculated adiabatic flame temperature is higher than at real conditions (Table 7), and the difference is dependent on the heat loss tendency from the reaction system to the surroundings. Clearly, the larger the heat losses, the higher the lower flammability limit, where to reach the lower limit flame temperature, more fuel combustion is needed to offset heat losses.

Finally, it is valuable to compare the results of CFT modeling with Le Chatelier's Law. Le Chatelier's Law is the simplest method to predict fuel mixture lower flammability limits on an empirical basis. CFT modeling is developed on the principle of energy and mass conservation, and it provides a different approach to predict the lower flammability limits of fuel mixtures. Figs. 8–12 represent the comparison of results for different binary hydrocarbon mixtures and illustrate the consistency between CFT modeling results and Le Chatelier's Law predictions. Mashuga and Crowl [23] gave a theoretical derivation of Le Chatelier's Law with certain assumptions, which include adiabatic conditions, constant flame temperature, constant heat capacities of reaction products, and constant number of moles of gas. Because CFT modeling is a theoretical approach to predict the lower flammability limits of fuel mixture, in some

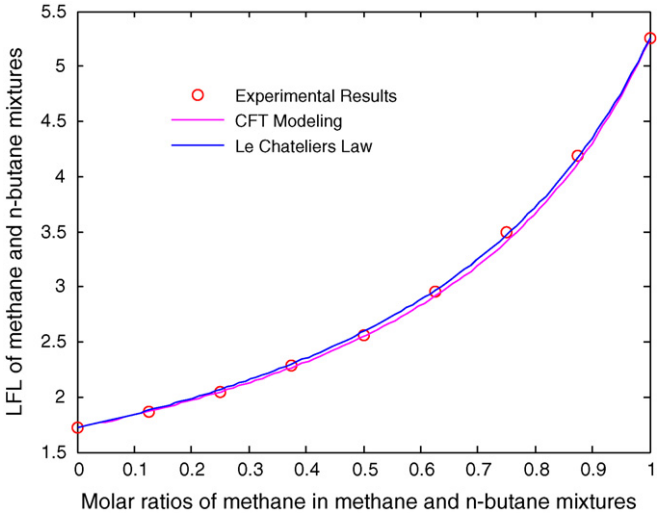

Fig. 9. LFL estimations for methane and *n*-butane mixtures using CFT modeling and Le Chatelier's Law.

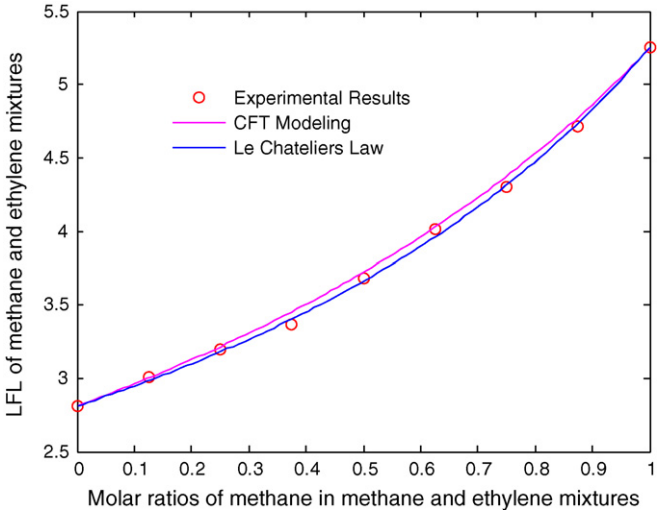

Fig. 10. LFL estimations for methane and ethylene mixtures using CFT modeling and Le Chatelier's Law.

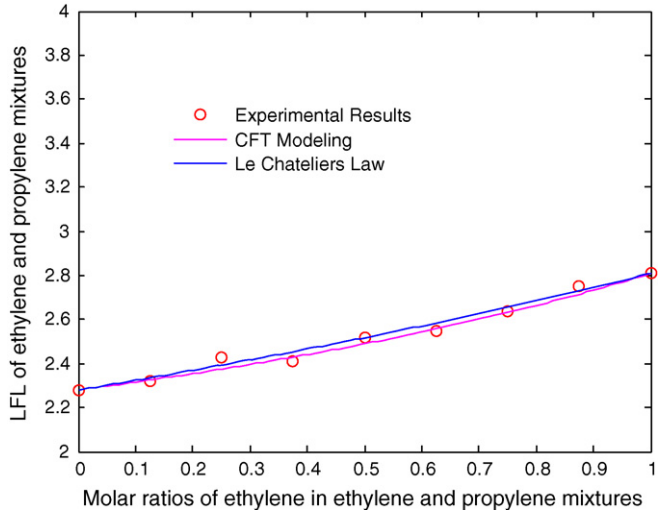

Fig. 11. LFL estimations for ethylene and propylene mixtures using CFT modeling and Le Chatelier's Law.

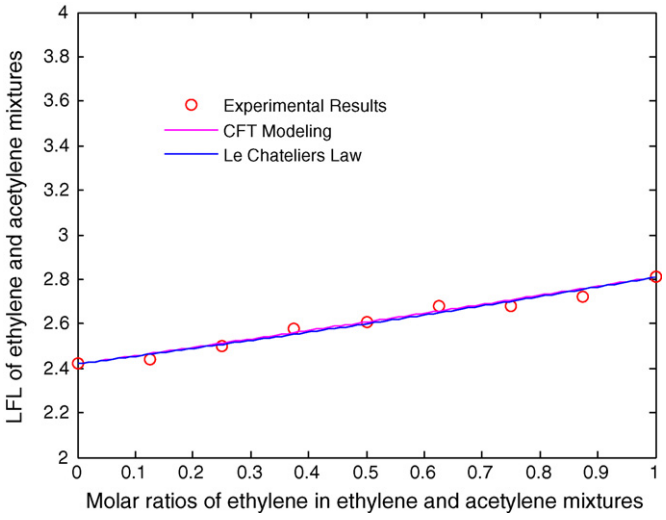

Fig. 12. LFL estimations for ethylene and acetylene mixtures using CFT modeling and Le Chatelier's Law.

sense, it provides another theoretical explanation of Le Chatelier's Law with no limitation from Mashuga's assumptions.

5. Conclusions

Of all the parameters that affect flammability limit estimation, heat loss is indispensable when the quenching effect becomes significant in the flammability apparatus. Different from CAFT modeling under the assumption of adiabatic conditions, a non-ideal flame temperature method, CFT modeling, is constructed and it involves a four-step procedure:

(i) Collecting pure fuel lower flammability limit data, which are specified to a certain apparatus;
(ii) Estimating the average flame temperature of the burned gas for pure fuels;
(iii) Estimating the average flame temperature of the burned gas for fuel mixtures;
(iv) Determining the lower flammability limits for the fuel mixtures.

CFT modeling is applied to predict the lower flammability limits of binary hydrocarbon mixtures (methane/propane, methane/*n*-butane, methane/ethylene, ethylene/propylene, and ethylene/acetylene). To verify the validity of CFT modeling, the prediction results were compared with experimental observations, and the minor deviations between them indicated that CFT modeling can represent experimental data very well.

Consistent predicted results of hydrocarbon mixture lower flammability limits from CFT modeling and Le Chatelier's Law indicate that CFT modeling, in some sense, provides a theoretical explanation of Le Chatelier's Law.

Acknowledgements

This research was sponsored by the Mary Kay O'Connor Process Safety Center, Artie McFerrin Department of Chemical Engineering, Texas A&M University.

References

[1] D.A. Crowl, J.F. Louvar, Chemical Process Safety-Fundamentals with Application, 2nd ed., Prentice Hall, 2002.
[2] J. Bond, Sources of ignition, in: Flammability Characteristics of Chemicals and Products, Butterworth-Heinemann Ltd, Oxford, 1991.
[3] L.G. Britton, Two hundred years of flammable limits, Process Safety Progress 21 (2002) 1–11.
[4] H.F. Coward, G.W. Jones, Limits of flammability of gases and vapors, Bulletin 503, Bureau of Mines, (1952).
[5] M.G. Zabetakis, Flammability characteristics of combustible gases and vapors, Bulletin 627, Bureau of Mines, (1965).
[6] Y. Shoshin, L. Tecce, J. Jarosinski, Experimental and computational study of lean limit methane-air flame propagating upward in a 24 mm diameter tube, Combustion Science and Technology 180 (2008) 1812–1828.
[7] A. Takahashi, Y. Urano, K. Tokuhashi, S. Kondo, Effect of vessel size and shape on experimental flammability limit of gases, Journal of Hazardous Materials A105 (2003) 27–37.
[8] T.A. Albahri, Flammability characteristics of pure hydrocarbons, Chemical Engineering Science 58 (2003) 3629–3641.
[9] Y.N. Shebeko, W. Fan, I.A. Bolodian, V.Y. Navzenya, An analytical evaluation of flammability limits of gaseous mixtures of combustible-oxidizer-diluent, Fire Safety Journal 37 (2002) 549–568.
[10] M. Vidal, W. Wong, W.J. Rogers, M.S. Mannan, Evaluation of lower flammability limits of fuel-air-diluent mixtures using calculated adiabatic flame temperature, Journal of Hazardous Materials 130 (2006) 21–27.
[11] W.K. Wong, Measurement of flammability in a closed cylindrical vessel with thermal criterion, Department of Chemical Engineering Texas A&M University, Texas, 2006.
[12] F. Zhao, W.J. Rogers, M.S. Mannan, Experimental measurement and numerical analysis of binary hydrocarbon mixture flammability limits, Process Safety and Environmental Protection 87 (2009) 94–104.
[13] I. Wierzba, G.A. Karim, H. Cheng, The flammability of rich gaseous fuel mixtures including those containing propane in air, Journal of Hazardous Materials 20 (1988) 303–312.
[14] D. Drysdale, An introduction to fire dynamics, in: Fire Science and Combustion, John Wiley and Sons, 1985.
[15] S.R. Turns, An introduction to combustion-concepts and application, in: Laminar Premixed Flames, 2nd ed, McGraw-Hill, 2000.
[16] A.G. Gaydon, H.G. Wolfhard, Flames-Their Structure, Radiation and Temperature, 4th Ed., Chapman and Hall, London, 1979.
[17] D. Drysdale, An introduction to fire dynamics, in: Limits of Flammability and Premixed Flames, John Wiley and Sons, 1985.
[18] E. Meyer, A theory of flame propagation limits due to heat loss, Combustion and Flame 1 (1957) 438–452.
[19] F.P. Incropera, D.P. Dewitt, T.L. Bergman, A.S. Lavine, Fundamentals of Heat and Mass Transfer, 6th ed., John Wiley and Sons, 2007.
[20] H.C. Hottel, A.F. Sarofim, Radiative transfer, in: Gas Emissivities and Absorptivities, McGraw-Hill, 1967.
[21] M.R. Brooks, D.A. Crowl, Flammability envelopes for methanol, ethanol, acetonitrile and toluene, Journal of Loss Prevention 20 (2007) 144–150.
[22] R. Chang, Chemistry, in: Thermochemistry, 9th ed., McGraw-Hill, 2007.
[23] C.V. Mashuga, D.A. Crowl, Derivation of Le Chatelier's mixing rule for flammable limits, Process Safety Progress 19 (2000) 112–117.